

Photomechanical Degrafting of Azo-Functionalized Poly(methacrylic acid) (PMAA) Brushes

Christian Schuh,[†] Nino Lomadze,[†] Jürgen Rühe,[†] Alexey Kopyshev,[‡] and Svetlana Santer^{*,†,§}

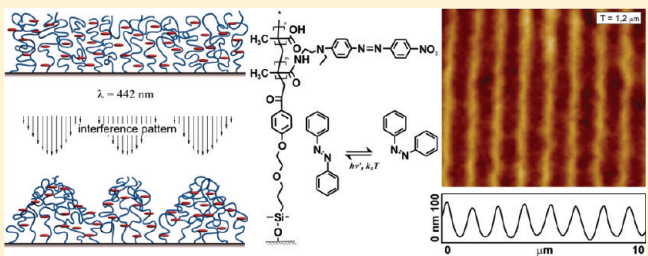
[†]Department of Microsystems Engineering (IMTEK), University of Freiburg, 79110 Freiburg, Germany

[‡]Institute of Advanced Studies (FRIAS), University of Freiburg, 79104 Freiburg, Germany

[§]Institute of Physics and Astronomy, University of Potsdam, 14476 Potsdam, Germany

Supporting Information

ABSTRACT: We report on the preparation and characterization of photosensitive polymer brushes. The brushes are synthesized through polymer analogous attachment of azo-benzene groups to surface-attached poly(methacrylic acid) (PMAA) chains. The topography of the photosensitive brushes shows a strong reaction upon irradiation with UV light. While homogeneous illumination leaves the polymer topography unchanged, irradiation of the samples with interference patterns with periodically varying light intensity leads to the formation of surface relief gratings (SRG). The height of the stripes of the grating can be controlled by adjusting the irradiation time. The SRG pattern can be erased through solvent treatment when the periodicity of the stripe pattern is less than the length of the fully stretched polymer chains. In the opposite case, photomechanical scission of receding polymer chains is observed during SRG formation, and the inscribed patterns are permanent.



INTRODUCTION

Azo-modified photosensitive polymer materials have received much attention over the last several decades.¹ Upon UV irradiation, azo-benzene molecules undergo reversible transitions from trans- to cis-configurations that can be reconverted to the thermodynamically more stable trans- configuration by light or heat.^{2–6} When the azobenzene moieties are attached to a polymer, the photoisomerization reaction affects the properties of the polymer over several length scales.^{7–12} Because of the different bonding angles of the double bond in the cis and trans form, both the length and the shape of the photosensitive molecules change considerably, so that for the cis configuration more free volume is required. In addition the dipole moment of the azo-group changes from ~ 0 D for the (thermodynamically more stable) trans-configuration to ~ 3 D for the cis-isomer. Because of these peculiar properties, the azobenzene-group containing polymers are successfully used to produce alignment layers for liquid crystalline fluorescent polymers in the display and semiconductor technology.^{13,14} Other examples for possible applications are components for waveguides and waveguide couplers^{15,16} or use as data storage media^{17–26} or as labels in quality product protection.^{27–31}

Among the many unusual physical phenomena related to azo-modified polymers is the formation of so-called surface relief gratings (SRG) upon irradiation with an interference pattern.^{32–35} In this process the UV light induces motion of polymer chains so that, depending on the local light intensity, in some areas of the substrate polymer is accumulated, while in others material

depletion occurs. This UV light-induced material flow can even occur at room temperature in air, that is, in the glassy state, where without UV irradiation the polymer behaves like a typical solid.^{36,37} This is interesting, as not only the local properties of the azo groups are changed, but the whole matrix and polymer structure changes itself.

Recently, UV induced flow in physisorbed photosensitive polymer films has been investigated to some extent, and several empirical models^{38–45} have been proposed to characterize the inscribing forces. A very promising hypothesis has been proposed in that the azo-molecules form distinct phases characterized by the orientation of the molecules in the exciting optical field.^{46,47} Morphological changes may then be explained, for instance, either by significant elastic strain induced in the regions of maximum light intensity or by a kind of condensation reaction where oriented phases grow and thereby attract polymer material which is dragged along.

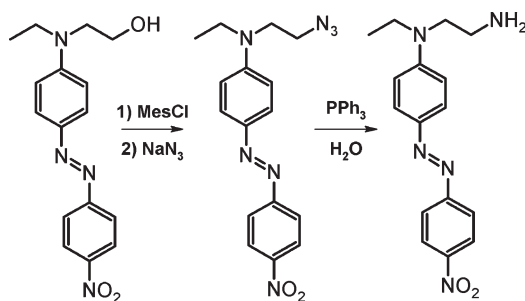
In this respect, it may prove useful to also consider other thin film molecular geometries such as polymer brushes that can provide significant preorientation of azo-molecules. It has been shown by Seki^{48,49} that attaching azobenzene groups to a brush leads to preferential orientation of the azo moieties parallel to the substrate. This can be understood by the extraordinary constraints that are put on the side chains in the brush configuration,

Received: May 4, 2011

Revised: July 7, 2011

Published: July 26, 2011

Scheme 1. Synthesis of DR-1 Amine Starting from Commercially Available DR-1



where the chains are covalently linked to the solid substrate at high grafting density and stretch away from it due to steric interactions with neighboring chains. In addition to the side chain orientation the brush backbone has a higher ground state free energy, because chains are under strong tension due to chain stretching. In this and other respects photosensitive polymer brushes may possibly show a much stronger response upon UV irradiation, also due to the rich phase separation behavior.

In this work we have extensively studied different types of thin photosensitive films consisting of polymers with azo-moieties as side groups. It turned out that there are indeed striking photo-mechanical differences between physisorbed films and brushes. Taking two comparable polymer films (same azo-content, molecular weight of the carrying polymer, and film thickness), there is a considerable difference in the photoinduced mobility of polymer material and the overall light-induced change in morphology. According to our results, it should be much more intense and even much faster than in physisorbed films. That is, in regions of UV intensity extremum, the polymer is almost completely removed, indicating that the covalent anchors are ruptured. This process is investigated as a function of irradiation time and the periodicity (length of a period) of the intensity pattern.

The scission process is interesting by itself, because it points to a thermodynamic nature of the forces acting on single chains similarly to those reported for scission in cylindrical brushes or thermal degradation in planar.^{50,51} The investigation of photo-mechanically induced rupturing of azo-modified polymer chains may eventually be helpful for a closer understanding of the phase separation behavior in photosensitive polymer films.

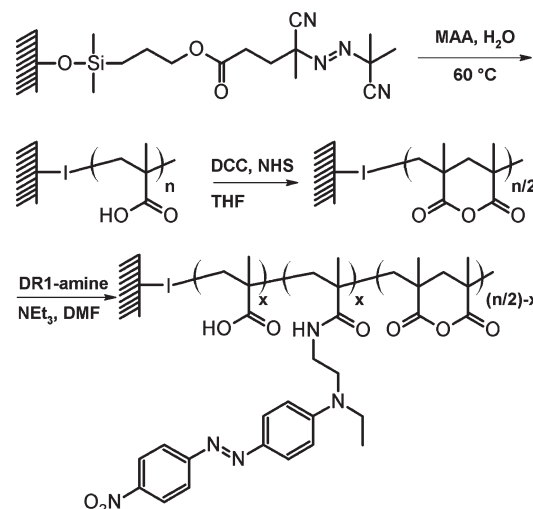
■ EXPERIMENTAL SECTION

Synthesis of Azo-PMAA Brushes. *Synthesis of DR-1 Amine.* The desired disperse-red 1 (DR-1) amine product was obtained in a Staudinger reaction with triphenylphosphine followed by a hydrolysis of the intermediary formed phosphinimine (Scheme 1), as described elsewhere.⁵²

Synthesis of PMAA Brushes. The poly(methacrylic acid) (PMAA) brushes were prepared by surface radical polymerization of MAA monomers using an immobilized azomonochlorosilane (AMCS) initiator on the substrate (“grafting from”) as depicted in Scheme 2.⁵³ After the polymerization step, all nonattached polymers were removed by extraction of the sample with methanol.

Coupling of DR-1 Amine with PMAA Chains. The activation of the PMAA brushes was accomplished with dicyclohexylcarbodiimide and *N*-hydroxysuccinimide in tetrahydrofuran (THF)

Scheme 2. Scheme of the Attachment of DR-1 to the PMAA Brush^a



^a First, PMAA brushes are grown from surface-attached initiators by a radical polymerization. The brushes are then activated by the quantitative transformation of n acid groups to $n/2$ anhydride groups. In the last step DR-1 amine reacts with the anhydride creating an equal amount of acid groups in the brush. Depending on the conversion of anhydride groups, the final brush consists equally of x acid and DR-1 amide groups and non-reacted anhydrides $(n/2) - x$.

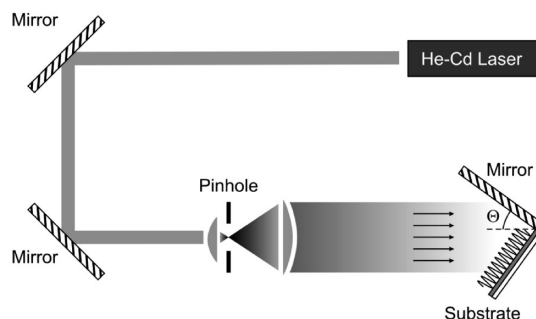


Figure 1. Scheme of the Lloyd's setup used for structuring photosensitive polymer brushes.

for 16 h. The activated surfaces were cleaned with methanol and dimethylformamide (DMF) and dried with a jet of nitrogen. The attachment of the amino-functionalized dye proceeded in DMF in the presence of 50 μ L of triethylamine. Depending on the desired amount of incorporated dye molecules, the reaction time was varied from a few seconds up to 7 h.

■ METHODS

Transmission Fourier transform infrared (FT-IR) spectra of the attached polymer layers were recorded using a Bio-Rad Excalibur spectrometer. The characterization of surface topography of azo-doped PMAA brushes was carried out with atomic force microscopy (AFM) (Nanoscope IIIa, Digital Instruments). The microscope was operated in tapping mode, using commercial tips (NanoSensors) with a resonance frequency of \sim 300 kHz, and a spring constant of \sim 50 N/m. The AFM micrographs were recorded in air at a temperature of around 23 °C.

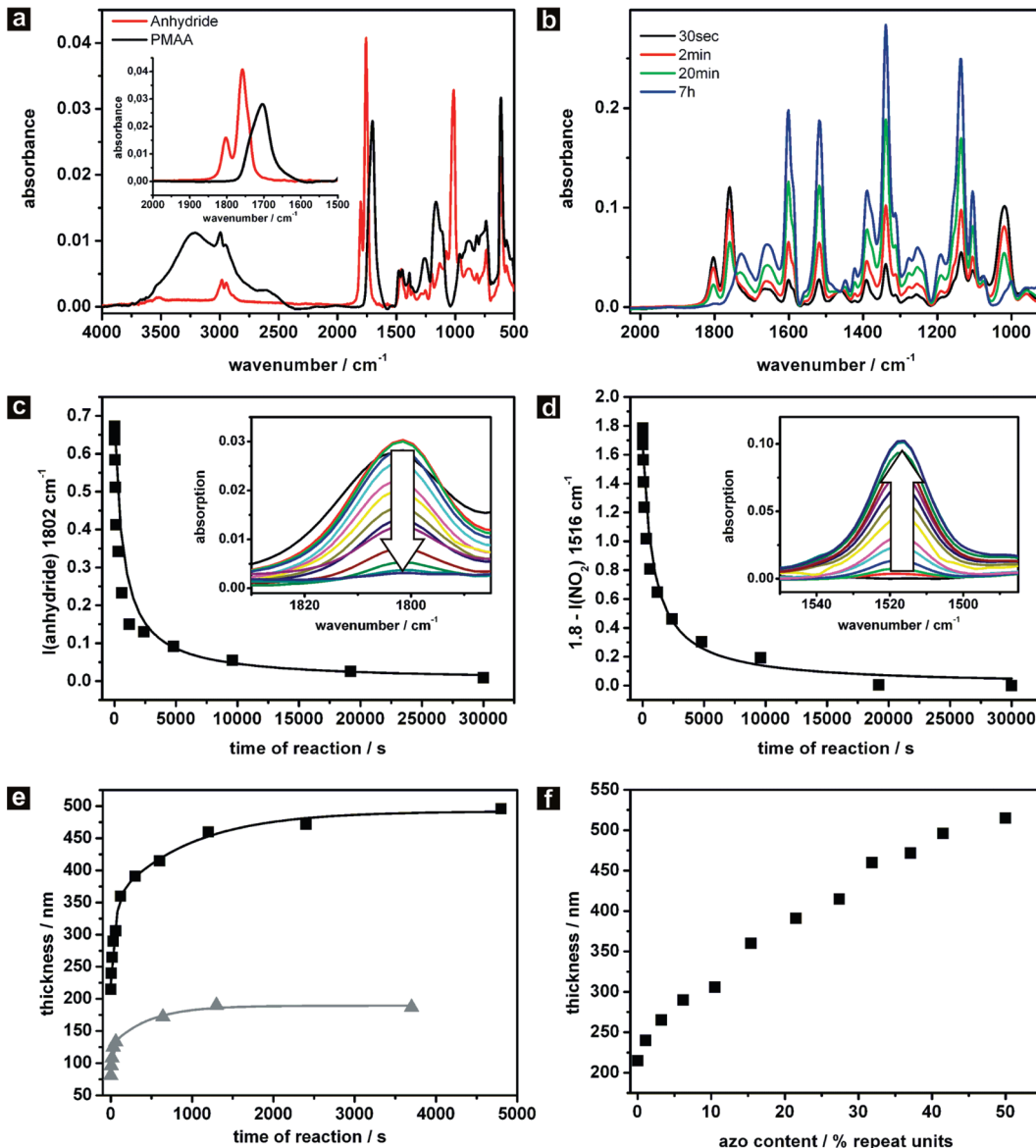


Figure 2. (a) FT-IR spectra of a PMAA brush (black line) and the corresponding anhydride brush (red line). (b) FT-IR spectra of activated brushes in contact with DR-1-amine for 30 s (black line), 2 min (red line), 20 min (green line), and 7 h (blue line). (c) Decrease of the anhydride signal area as a function of the reaction time. (d) Inverted signal of the increase of the nitro signal area as a function of reaction time. The black lines in c and d correspond to fits of second-order kinetics. (e) Evolution of dry thickness for two brushes with different starting thickness over the process of amidation. (f) Brush thickness as a function of the azo content derived from the increase of the nitro signal.

The Lloyd's mirror scheme with He–Cd laser (Kimmon) operating at $\lambda = 442$ nm (total power of about 60 mW) was used as UV interference lithography setup (Figure 1).

The beam of circularly polarized light is cleaned by a lens–pinhole unit and then split into two coherent beams by a mirror, interfering at the sample position to create a regular line pattern. The periodicity of the interference pattern is given by $d = \lambda / \sin(\theta/2)$, where λ is the wavelength of the incident light and θ is the angle between the incoming laser beam and the mirror surface. Irradiation times vary between several minutes and 2 h.

RESULTS AND DISCUSSION

To obtain a photosensitive polymer brush, the dye DR-1 was covalently attached to PMAA brushes using a three-step

synthetic procedure as described schematically in Scheme 2. The brushes were synthesized as previously reported through surface-initiated radical polymerization from a self-assembled monolayer of azoinitiators.⁵⁴ The carboxylic acid groups in the brushes were activated using carbodiimide chemistry in the presence of *N*-hydroxysuccinimide.⁵⁵ The reaction led to the corresponding anhydride in quantitative yields and not to the active ester product as one might have anticipated. The FT-IR spectra displayed in Figure 2a show that the vibrational bands at 3225 cm⁻¹ and 1705 cm⁻¹, which can be attributed to –OH and C=O bond in the acid completely disappear, indicating complete conversion (at least within the limits of infrared spectroscopy). In the product spectrum (red line) a new double peak at 1752 cm⁻¹ and 1805 cm⁻¹ appears that can be assigned to the anhydride. As the signal of the anhydride double peak at lower

Table 1. Molecular Parameters of Photosensitive Polymer Brushes Discussed in the Paper^a

| | I | II | III |
|---------------------------------------|-------------------|--------------------|-------------------|
| M_n^{PMAA} , g/mol | 5.5×10^5 | 1.85×10^6 | 2.2×10^6 |
| σ , $\mu\text{mol}/\text{m}^2$ | 0.27 | 0.042 | 0.118 |
| h_0^{PMAA} , nm | 190 ± 5 | 65 ± 5 | 235 ± 5 |
| azo content, % | 14 | 32 | 50 |
| h^{azo} , nm | 125 ± 5 | 72 ± 5 | 515 ± 5 |

^a M_n^{PMAA} is the number average molecular weight of the PMAA chains of the brush. σ is the calculated grafting density. h_0^{PMAA} and h^{azo} are the dry thickness of the bare brush and azo-modified one, respectively, as measured by AFM. The azo content is the percentage of the monomer units within a single PMAA chain substituted by the azo-side groups.

wave numbers has a higher intensity, one might conclude that preferentially intramolecular anhydride formation occurs. However, intermolecular reactions are also expected simply for statistical reasons.^{56,57}

These activated brushes were used in amidation reactions with disperse red 1 amine (DR-1 amine) (Scheme 2). The kinetics of the reaction was followed by FT-IR analysis (Figure 2b) through the decrease of the anhydride signal at 1803 cm^{-1} (Figure 2c) and the increase of the $-\text{NO}_2$ vibrational band of DR-1 at 1517 cm^{-1} (Figure 2d). As a second method the brush (dry) thickness, which increases due to the molecular weight increase as a consequence of addition of the azo compound, was measured by AFM (Figure 2e).

To get information on the rate constants of the reaction, the obtained data were fitted with second-order kinetics:

$$[\text{A}] = \frac{[\text{A}_0]}{1 + kt[\text{A}_0]}$$

This was done both for the decrease of the anhydride signal as well as for the increase of the nitro signal which was plotted inverted for the fitting (Figure 2c,d). The values of k for both fits have similar values ($k = 2.0 \times 10^{-3} \text{ s}^{-1}$ for the anhydride signal and $k = 1.7 \times 10^{-3} \text{ s}^{-1}$ for the nitro signal) and result in a half-life time of $t_{1/2} = 356 \text{ s}$.

As the molecular weight of the repeat units increases quite strongly by adding the azo units from 86 g/mol for the acid to 467.2 g/mol (for maximum conversion, i.e., 50% azo contents), the (dry) thickness of a given MAA brush depends strongly on the degree of functionalization with the azo side chains. The evolution of the thickness of the brush as a function of reaction time is depicted in Figure 2e and as a function of the amount of repeat units carrying a dye in Figure 2f. At 100% conversion the final brush should consist of 50% MAA and 50% DR-1 amide repeat units. The initial height of the PMAA brush shown in Figure 2f and measured using the AFM scratching procedure was $236 \pm 10 \text{ nm}$. Assuming that the molecular weight of the free polymer and that of the brush are the same, the grafting density of the MAA brush was calculated to $0.118 \mu\text{mol}/\text{m}^2$. Using these data and the equation $M_n = (\sigma d)/\rho$, where d is the brush height, ρ is the density of the PMAA polymer to be 0.9 g/cm^3 , and σ is the grafting density, we can estimate the number average molecular weight of the polymer chains. Under the assumption that the grafting density (i.e., no chains are degrafted during the functionalization) and the density of the material remains constant, the increase in molecular weight should lead at maximum to a 2.9 fold increase in the dry thickness (100% conversion and

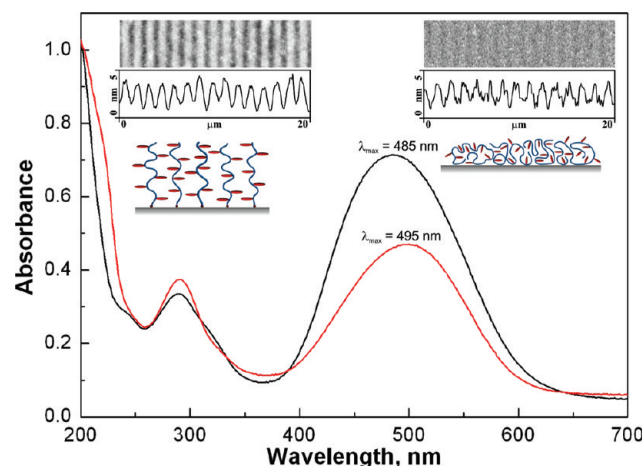


Figure 3. (a) UV absorption spectra of azo-PMAA chains (50% of azo within the chain) in brush configuration (black line) and in the physisorbed layer (red curve). (b and c) AFM micrographs of the topography of polymer brush and polymer film, respectively, after irradiation with the UV interference pattern for 2 min and 1 h at $\lambda = 442 \text{ nm}$. A schematic representation of the suggested orientation of azo-side groups within the layer is inserted.

accordingly 50% functionalization). In our experiments we could observe a 2.3 fold increase in the brush dry thickness for both cases. Deviations from the expected value can be explained with variations of the density of the material which we did not take into account.

The amount of incorporated azo dye was calculated from the ratio of the nitro to anhydride signal in the FT-IR spectra using a calibration curve (see Supporting Information).

In the following, we will discuss the functionalization of three brushes whose molecular parameters are summarized in Table 1.

Irradiation of the azo-PMAA brush with azo contents 50% with a UV interference pattern at $\lambda = 442 \text{ nm}$ for 2 min results in the formation of topography pattern corresponding to the light intensity distribution [surface relief grating (SRG)] (Figure 3). The stripes formed have a height of 5 nm and a periodicity of 1.2 μm . To compare the photosensitive brush with a corresponding physisorbed film, we have collected PMAA chains formed as free polymer during the synthesis of the brush. The PMAA chains were then modified with the azo dye as described above and drop-casted on a glass substrate. This process guarantees that the polymer in the brushes and the physisorbed layers have similar molecular weights and polydispersities. The cast film has a flat topography with the root-mean-square (rms) roughness of 0.8 nm over an area of $10 \mu\text{m} \times 10 \mu\text{m}$. By choosing the appropriate concentration the thickness of the film is adjusted close to 500 nm, comparable to the brush thickness. The kinetics of stripe formation within the physisorbed film is much slower as compared to the brush. To increase the stripe height by 5 nm, 1 h of irradiation was necessary. This strong difference in the kinetics is most likely due to a preferential orientation of azo-groups within the brush. According to the previous studies of the brushes with a liquid crystalline-like structure,^{18,58,59} this should be expected as, due to the orientation of the main chain, the azo-group side chains should preferentially align parallel to the surface (Figure 3a, insert). As the incident light was polarized parallel to the surface, a large probability of light absorbing is expected, as it is a quadratic function of the cosine of the angle

between the electrical field vector and the main axis of the azo-group. In contrast, in the physisorbed films there is no preferential orientation of azo groups (see inserted scheme in Figure 3b) so that a certain portion fraction will have an orientation perpendicular to the polarization of incoming light, leaving them optically inactive. Figure 3 parts c and d show UV absorption spectra of the azo-PMAA brush and the physisorbed film, respectively. The peaks around 285 and 490 nm were assigned to the $\varphi-\varphi^*$ transition of the aromatic ring^{60,61} and $\pi-\pi^*$ long-axis transitions of the azo-group, respectively. A slight hypsochromic peak shift was observed for the $\pi-\pi^*$ absorption band of the polymer brush (485 nm) compared to that of the physisorbed film (495 nm), indicating more H-aggregates and thus higher order in the brush.

It should be noted that it was possible to erase the stripes written into the brush by short treatment with a good solvent (DMF). The residual variations in height are only about 0.5 nm and thus of the order of the film roughness. The reason for such a residual morphology may be a slight, partial alignment of the azo groups resulting in a corresponding density change. This can also be inferred from AFM phase micrographs where the phase contrast at such a small height variation is a strong indication

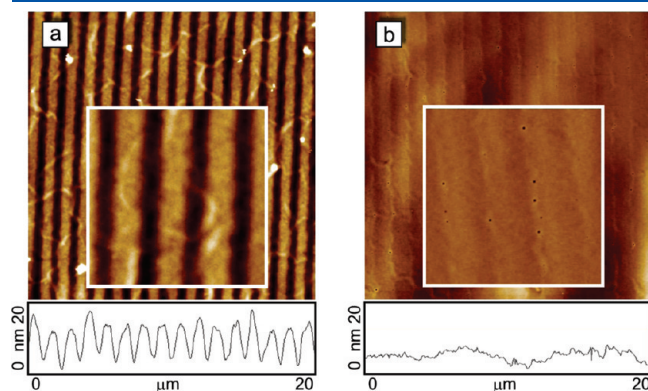


Figure 4. (a) AFM micrograph of the azo-PMAA brush (50% of DR-1) after UV irradiation at $\lambda = 442$ nm during 5 min with the interference pattern of $1.2\ \mu\text{m}$ periodicity. (b) The same area after treatment with DMF solvent during 1 min.

of a difference in material density. In contrast, when a physisorbed film was irradiated and solvent treated under the same conditions, the whole film was completely removed (Figure 4).

It should be noted that the discussion above refers to the case when the length of a polymer chain is larger than the periodicity length of the interference pattern. The contour length l_{contour} of the fully stretched chain is for the given molecular weight ($M_n = 2.2 \times 10^6$ g/mol, DP = 26.000) around $6\ \mu\text{m}$. In this case, the brush morphology can be returned to an almost flat topography.

The situation is quite different when the length of the polymer chain is smaller or comparable to the periodicity length of the interference pattern. As an example, a PMAA brush with a molecular weight of 5.5×10^5 g/mol, which has a contour length of $1.3\ \mu\text{m}$, was chosen. When the brush was irradiated under the same conditions (at $\lambda = 442$ nm and periodicity length of $1.2\ \mu\text{m}$, for 1 min), stripes of 2 nm in height were formed (Figure 5a), but the subsequent treatment with the DMF solvent does not lead back to the initially flat structure. The height of the stripes increases even further up to 6 nm (Figure 5b).

After irradiating for 2 min, the stripes height increases to 4 nm, and after treatment with DMF the height of the grating was 60 nm (Figure 5c). However, when the same brush was used and the periodicity of the interference pattern was decreased by a factor of 2 (660 nm), scission does not occur, as shown in Figure 5 parts d and e. The stripe height rises to 4 nm as in the case of large periodicity (Figure 4c), but by treating the sample with DMF, the topography returns to a rather flat state, without noticeable loss of polymer chains. Again, the residual variations in the topography, which had an amplitude of less than 1 nm, could well be assigned to the change in the density of the material resulting from alignment of the azo side chains during irradiation. Further annealing of the brush in the solvent over 48 h results in a completely flat topography. In Figure 6 we show how the stripe depth depends on the periodicity of the interference pattern.

It is interesting that, at larger distances between neighboring stripes (minima of interference pattern), the stripe depth increases considerably. This is surprising at first sight, since the mobility of the polymer should be quite strongly restricted due to the covalent attachment to the substrate, and one does not expect such an increase, especially if the polymer chain is short compared to the interstripe distance. This suggests the following

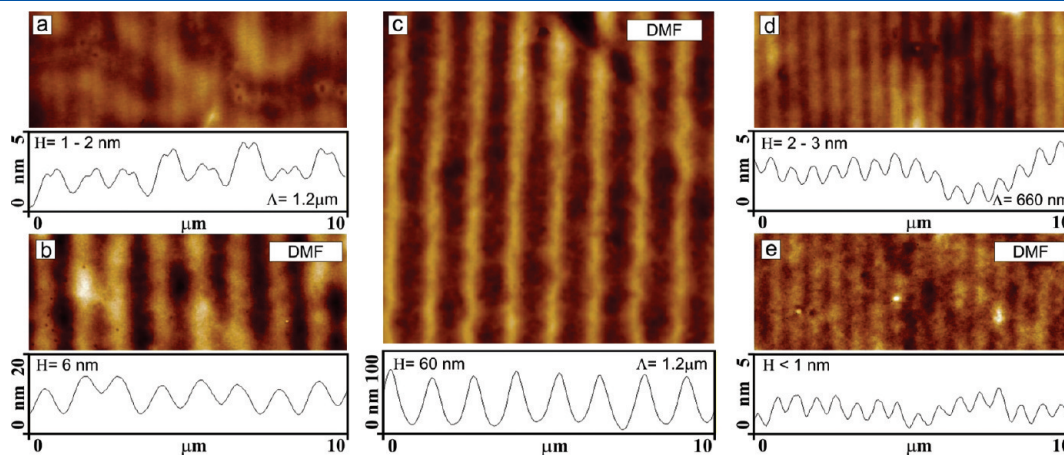


Figure 5. AFM micrographs of the azo-PMAA brush (14% DR-1) after irradiation with UV light ($\lambda = 442$ nm) for 1 min (a) and after subsequent treatment with DMF (b); (c) the topography of a similar sample as in b after 2 min irradiation and treatment with DMF. The height of the stripes increases in this case from 4 nm after irradiation to 60 nm after exposure to DMF. (d) Decreasing the periodicity of the interference pattern to 660 nm does not influence the height of the stripes after irradiation, but treatment with DMF does not result in height increases (e).

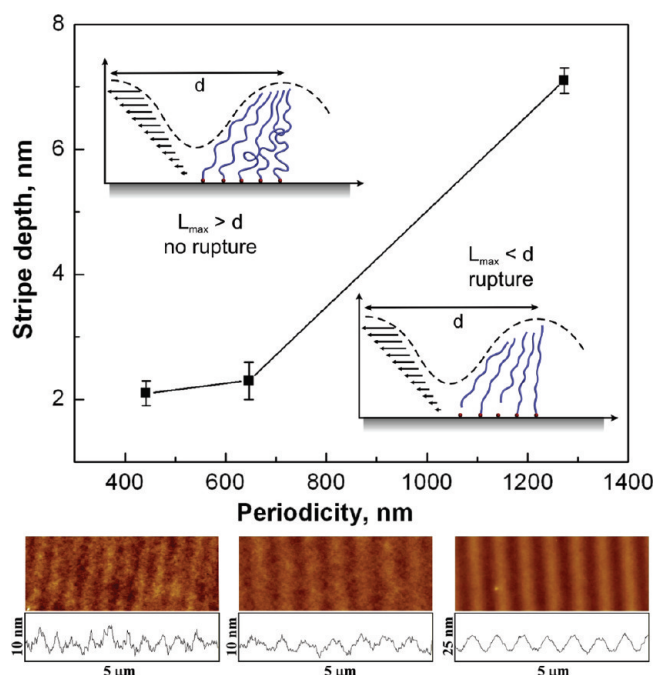


Figure 6. Stripe depth of the brush (I from the Table 1) after treatment with a good solvent as a function of the length of the period of the interference pattern and corresponding AFM micrographs; irradiation time 1 min at $\lambda = 442$ nm). The schematic diagrams illustrate how the scission process, occurring at larger periodicity lengths, can be pictured: at small stripe distance the chains are not fully extended when the mass transport ceases. At greater distances, the chains are fully stretched before mass transport is completed and eventually detach from the substrate.

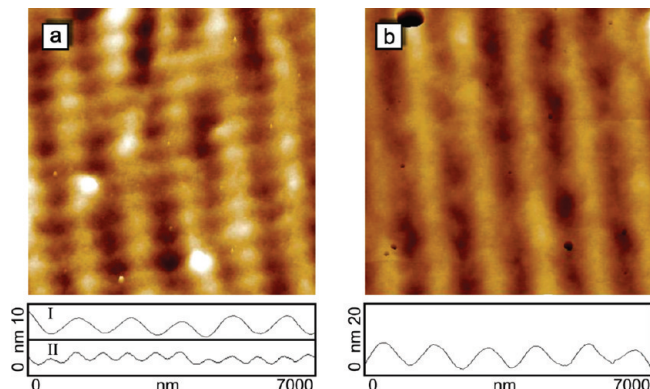


Figure 7. (a) AFM micrographs of the cross irradiated brush topography. After first irradiation, the brush was rinsed with good solvent to remove the ruptured chains followed by irradiation with a crossed intensity pattern. (b) The brush was rinsed with DMF resulting in erasure of the second grating.

interpretation: during mass transport induced by UV irradiation, the forces on the polymer chains causing the redistribution of the polymer exceed the strength of the covalent bonds, and significant rupture occurs during the morphology change. When the samples are treated with a good solvent for the polymer, the detached azo-PMAA chains are washed away, leaving a brush with stripes of lower grafting density in all areas where polymer material has receded. In areas of polymer mass accumulation

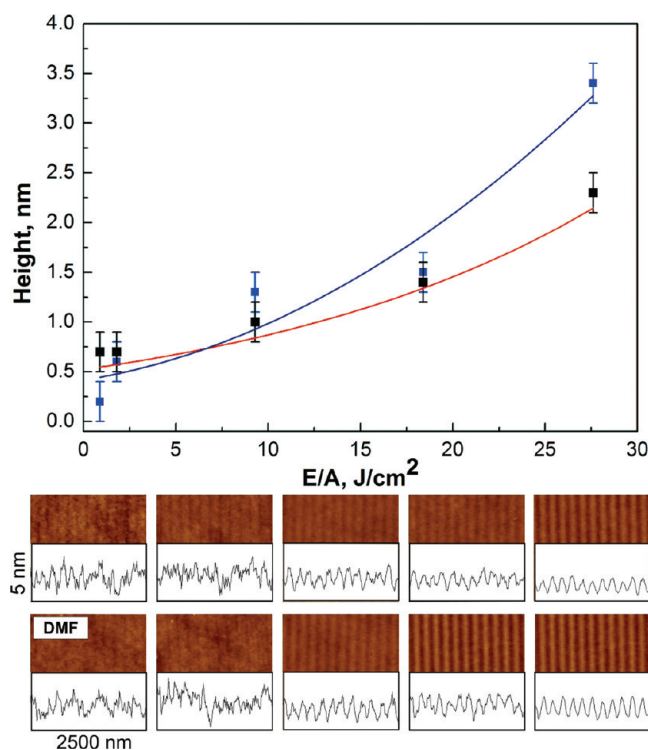


Figure 8. Stripe formation in the case of small periodicity length and longer irradiation time. The stripe depth is plotted against the total irradiation energy collected, in the case of small periodicity length (330 nm) and longer irradiation time. As the irradiation power is kept constant during the experiment, the energy is directly proportional to exposure time. As in the case of large periodicity length, the stripe depth assumes larger values on illumination after treatment with DMF (blue data points) than on illumination before (red data points). Even under long exposure time, the corresponding changes are rather small.

(the hills of the stripes) it seems that the grafting density remains unchanged as the layer thickness at the top of the stripes remains at its initial value. In other words, the increase in stripe height is due to a decrease in film thickness in the areas where the polymer has retreated.

Figure 7 shows the brush as described in Figure 5, after inscription of a permanent pattern. In a second step the sample was turned 90°, and irradiation with a lower periodicity of the interference pattern was performed directly on the brush after treatment with DMF. At an irradiation time of 2 min, the height of the stripes of lower periodicity was found again to be 4 nm as in the case of the initial irradiation. The treatment of the cross-irradiated brush with DMF erases the second grating of low periodicity, indicating the absence of scission of covalent bonds. The experiment shows that on the identical sample both reversible and permanent patterns can be inscribed simply by adjusting the size of the interference pattern for a given molecular weight.

It should be emphasized that chain rupture is only caused by mass transport and is not due to UV light-induced degradation. This was shown by irradiating the azo-PMAA brush for extended periods of time (1 h) with a homogeneous light intensity distribution. No change in brush thickness was observed neither directly after irradiation nor after additional treatment with DMF. Also the irradiation of the PMAA brush containing no azo dye with an interference pattern during 1 h does not lead to

changes in brush topography, ruling out a simple photodegradation of the polymer material. Only after 2 h of UV irradiation, stripes of 1 nm in height were observed in the PMAA brush. These two control experiments show that indeed mass transport and photodegrafting are the relevant processes in the azo-brushes.

The development of stripe depth against illumination time for the case of a low periodicity pattern is illustrated in Figure 8. With increasing illumination time the stripe height is slowly increased. At low irradiation times (i.e., low dose) no change in the pattern occurs after washing. At long irradiation times a small increase of the stripe height is observed during washing, indicating some chain rupture. This effect, however, is with 1–2 nm, very small in comparison to the corresponding results on illumination patterns with low periodicity, where under these circumstances practically all polymer material is removed from the “valleys”. This is not surprising as the light intensity pattern is not infinitely sharp, but rather sinusoidal in profile, and the polymer molecules have a certain polydispersity, so that longer and shorter chains coexist.

CONCLUSION

In this paper we reported on the photoinduced scission of azo-modified polymer brushes covalently linked to a solid surface. The photodegrafting process is caused by mass transport of the azopolymer induced by UV light with spatially varying intensity. The motion and relocation of azo dyes bound to the polymer induce stress in the polymer brushes. This stress can become so large under appropriate conditions that the backbone of the polymer chain breaks. The broken-off parts of the polymer chains can then move freely along the gradient in irradiation intensity. This together with reversible movement in some of the surface-attached chains generates locations with excess polymer, while in the areas of origin of the broken-off polymer chains the polymer film becomes thinner, leading to the formation of the typical surface relief gratings. The broken-off polymer can be washed away in subsequent solvent exposure. Critical factors for breaking the polymer chains seem to be the extent of photophysically induced tension and how far the polymer is transported. The latter is determined by the periodicity length of the intensity pattern in relation to the size of the polymer chains. When the travel distance is smaller than the average length of the polymer molecules, no chain breakage occurs, and reversible patterns are inscribed. The extent of polymer relocation depends on the degree of functionalization by the azo side groups and the irradiation time. If such patterned samples become annealed through solvent exposure, they return to the initial flat state.

If, however, the distance of the light-induced movement of the polymer (sub)chains is larger than the average length of the polymer molecules, some chains are ripped off of the areas from which they recede. When such an irradiated sample is washed with good solvent for the polymer, the layer thickness in the depleted areas is strongly decreased, whereas in those zones where polymer chains have entered, the original film thickness is regained after extraction. The inscription of such structures is then permanent.

As the figure of merit seems to be the ratio between grating periodicity and length of the polymer chains, reducing or increasing the molecular weight of the surface-attached chains has a very similar effect on the degrafting process. It is quite remarkable that, with the same chemistry and the same irradiation conditions depending on the ratio between grating periodicity and molecular weight of the surface-attached chains, either reversible or irreversible patterns can be generated.

In further studies it needs to be elucidated how the degrafting process is influenced by the grafting density of the surface-attached chains as prestretching of the polymer chains could influence the stability of the polymer molecules. In addition, the activation energies of the chain-breaking process can be determined from the degrafting kinetics, which in turn allows us to estimate the energy and accordingly the forces induced by the isomerization of the azo groups.

ASSOCIATED CONTENT

S Supporting Information. FT-IR calibration curve and description. This material is available free of charge via the Internet at <http://pubs.acs.org>.

AUTHOR INFORMATION

Corresponding Author

*E-mail address: santer@uni-potsdam.de.

ACKNOWLEDGMENT

This research is supported by the DFG (SA1657/3-1). We thank Dr. Wolfgang Mönch and Bernd Aatz for their support with the laser setup.

REFERENCES

- (1) Zhao, Y.; Ikeada, T., Eds. *Smart Light-Responsive Materials: Azobenzene-Containing Polymers and Liquid Crystals*; John Wiley: Hoboken, NJ, 2009.
- (2) Rau, H. In *Photochemistry and Photophysics*; Rebek, J., Ed.; CRC Press: Boca Raton, FL, 1990; Vol. 2, pp 119–141.
- (3) Todorov, T.; Nikolova, L.; Tomova, N. *Appl. Opt.* **1984**, *23*, 4309–4312.
- (4) Jones, C.; Day, S. *Nature* **1991**, *351*, 15.
- (5) Loucif-Saibi, R.; Nakatani, K.; Delaire, J. A.; Dumont, M.; Sekkat, Z. *Chem. Mater.* **1993**, *5*, 229–236.
- (6) Eich, M.; Wendorff, J. H. *Makromol. Chem. Rapid Commun.* **1987**, *8*, 467–471.
- (7) Sekkat, Z.; Knoll, W. *Photoreactive Organic Thin Films*; Academic Press: New York, 2002.
- (8) Zhao, Y.; He, J. *Soft Matter* **2009**, *5*, 2686–2693.
- (9) Yin, R.; Xu, W.; Kondo, M.; Yen, C.-C.; Mamiya, J.-I.; Ikeda, T.; Yu, Y. *J. Mater. Chem.* **2009**, *19*, 3141–3143.
- (10) Yamada, M.; Kondo, M.; Mamiya, J.-I.; Yu, Y.; Kinoshita, M.; Barrett, C. J.; Ikeda, T. *Angew. Chem., Int. Ed.* **2008**, *47*, 4986–4988.
- (11) Seki, T.; Nagano, S. *Chem. Lett.* **2008**, *37*, 484–489.
- (12) Natansohn, A.; Rochon, P. *Chem. Rev.* **2002**, *102*, 4139–4176.
- (13) Sainova, D.; Zen, A.; Nothofer, H.-G.; Asawapirom, U.; Scherf, U.; Hagen, R.; Bieringer, T.; Kostromine, S.; Neher, D. *Adv. Funct. Mater.* **2002**, *12*, 49–57.
- (14) Zen, A.; Neher, D.; Bauer, C.; Asawapirom, U.; Scherf, U.; Hagen, R.; Kostromine, S.; Mahrt, R. F. *Appl. Phys. Lett.* **2002**, *80*, 4699–4701.
- (15) Viswanathan, N. K.; Kim, D. Y.; Bian, S.; Williams, J.; Liu, W.; Li, L.; Samuelson, L.; Kumar, J.; Tripathy, S. K. *J. Mater. Chem.* **1999**, *9*, 1941–1955.
- (16) Natansohn, A.; Rochon, P. *Adv. Mater.* **1999**, *11*, 1387–1391.
- (17) Berg, R. H.; Hvilsted, S.; Ramanujam, P. S. *Nature* **1996**, *383*, 505–508.
- (18) Rasmussen, P. H.; Ramanujam, P. S.; Hvilsted, S.; Berg, R. H. *J. Am. Chem. Soc.* **1999**, *121*, 4738–4743.
- (19) Zilker, S. J.; Bieringer, T.; Haarer, D.; Stein, R. S.; van Egmond, J. W.; Kostromine, S. G. *Adv. Mater.* **1998**, *10*, 855–859.

- (20) Stracke, A.; Wendorff, J. H.; Goldmann, D.; Janietz, D.; Stiller, B. *Adv. Mater.* **2000**, *12*, 282–285.
- (21) Seki, T. *Bull. Chem. Soc. Jpn.* **2007**, *80*, 2084–2109.
- (22) Barrett, C. J.; Mamiya, J.; Yager, K. G.; Ikeda, T. *Soft Matter* **2007**, *3*, 1249–1261.
- (23) Ichimura, K. *Chem. Rev.* **2000**, *100*, 1847–1874.
- (24) Yager, K. G.; Barrett, C. J. *J. Photochem. Photobiol., A* **2006**, *182*, 250–261.
- (25) Yager, K. G.; Barrett, C. J. *Curr. Opin. Solid State Mater. Sci.* **2001**, *5*, 487–494.
- (26) Ichimura, K.; Oh, S. K.; Nakagawa, M. *Science* **2000**, *288*, 1624–1626.
- (27) Stiller, B.; Geue, T.; Morawetz, K.; Saphiannikova, M. *J. Microsc. Rev. Lett.* **2001**, *87*, 015501.
- (29) Yu, Y. L.; Nakano, M.; Ikeda, T. *Nature* **2003**, *425*, 145–145.
- (30) Reinhold, B.; Geue, T. M.; Morawetz, K.; Saphiannikova, M.; Grenzer, J.; Panzner, T.; Pietsch, U. *HASYLAB annual report*; HASY-LAB: Hamburg, 2002.
- (31) Yi, D. K.; Kim, M. J.; Kim, D.-Y. *Langmuir* **2002**, *18*, 2019–2023.
- (32) Rochon, P.; Batalla, E.; Natansohn, A. *Appl. Phys. Lett.* **1995**, *66*, 136–138.
- (33) Kim, D. Y.; Tripathy, S. K.; Li, L.; Kumar, J. *Appl. Phys. Lett.* **1995**, *66*, 1166–1168.
- (34) Barrett, C.; Rochon, P.; Natansohn, A. *J. Phys. Chem.* **1996**, *100*, 8836–8842.
- (35) Kim, D. Y.; Li, L.; Jiang, X. L.; Shivshankar, V.; Kumar, J.; Tripathy, S. K. *Macromolecules* **1995**, *28*, 8835–8839.
- (36) Tanchak, O. M.; Barrett, C. J. *Macromolecules* **2005**, *38*, 10566–10570.
- (37) Yager, K. G.; Tanchak, O. M.; Godbout, C.; Fritzsche, H.; Barrett, C. J. *Macromolecules* **2006**, *39*, 9311–9319.
- (38) Barrett, C. J.; Rochon, P. L.; Natansohn, A. L. *J. Chem. Phys.* **1998**, *109*, 1505–1516.
- (39) Kumar, J.; Li, L.; Jiang, X. L.; Kim, D.-Y.; Lee, T. S.; Tripathy, S. *Appl. Phys. Lett.* **1998**, *72*, 2096–2098.
- (40) Bian, S.; Williams, J. M.; Kim, D. Y.; Li, L.; Balasubramanian, S.; Kumar, J.; Tripathy, S. *J. Appl. Phys.* **1999**, *86*, 4498–4508.
- (41) Lefin, P.; Fiorini, C.; Nunzi, J.-M. *Pure Appl. Opt.* **1998**, *7*, 71–82.
- (42) Lefin, P.; Fiorini, C.; Nunzi, J. M. *Opt. Mater.* **1998**, *9*, 323–328.
- (43) Pedersen, T. G.; Johansen, P. M.; Holme, N. C. R.; Ramanujam, P. S.; Hvilsted, S. *Phys. Rev. Lett.* **1998**, *80*, 89–92.
- (44) Baldus, O.; Leopold, A.; Hagen, R.; Bieringer, T.; Zilker, S. J. *J. Chem. Phys.* **2001**, *114*, 1344–1349.
- (45) Baldus, O.; Zilker, S. J. *Appl. Phys. B: Laser Opt.* **2001**, *72*, 425–427.
- (46) Geue, T. M.; Saphiannikova, M. G.; Henneberg, O.; Pietsch, U.; Rochon, P. L.; Natansohn, A. L. *Phys. Rev. E* **2002**, *65*, 052801/4.
- (47) Saphiannikova, M.; Neher, D. *J. Phys. Chem. B* **2005**, *109*, 19428–19436.
- (48) Seki, T. *Curr. Opin. Solid State Mater. Sci.* **2006**, *10*, 241–248.
- (49) Uekusa, T.; Nagano, S.; Seki, T. *Macromolecules* **2009**, *42*, 312–318.
- (50) Lebedeva, N. V.; Sun, F. C.; Lee, H.; Matyjaszewski, K.; Sheiko, S. S. *J. Am. Chem. Soc.* **2008**, *130*, 4228–4229b.
- (51) Sheiko, S. S.; Sun, F. C.; Randall, A.; Shirvanyants, D.; Rubinstein, M.; Lee, H.; Matyjaszewski, K. *Nature* **2006**, *440*, 191–194.
- (52) Zhang, J.; Drugeon, G.; L'hermite, N. *Tetrahedron Lett.* **2001**, *42*, 3599–3601.
- (53) Prucker, O.; Rühe, J. *Langmuir* **1998**, *14*, 6893–6898.
- (54) Konradi, R.; Rühe, J. *Macromolecules* **2004**, *37*, 6954–6961.
- (55) Harris, B. P.; Kutty, J. K.; Fritz, E. W.; Webb, C. K.; Burg, K. J. L.; Metters, A. T. *Langmuir* **2006**, *22*, 4467–4471.
- (56) Scott, L. T.; Rebek, J.; Ovsyanko, L.; Sims, C. L. *J. Am. Chem. Soc.* **1977**, *99*, 625–626.
- (57) Gross, H.; Bilk, L. *Tetrahedron* **1968**, *24*, 6935–6939.
- (58) Peng, B.; Rühe, J.; Johannsmann, D. *Adv. Mater.* **2000**, *12*, 821–824.
- (59) Peng, B.; Johannsmann, D.; Rühe, J. *Macromolecules* **1999**, *32*, 6759–6766.
- (60) Fabian, J.; Hartmann, H. *Light Absorption of Organic Colorants*; Springer-Verlag: Berlin, 1980; pp 32–79.
- (61) Sapich, B.; Vix, A. B. E.; Rabe, J. P.; Stumpe, J.; Wilbert, G.; Zentel, R. *Thin Solid Films* **2006**, *514*, 165–173.